Anal Bioanal Chem (2015) 407:1735–1744
DOI 10.1007/s00216-014-8425-0

RESEARCH PAPER

Development and characterization of magnetic molecularly imprinted polymers for the selective enrichment of endocrine disrupting chemicals in water and milk samples

Xiaoyu Xie · Xiaoyan Pan · Shengli Han · Sicen Wang

Received: 30 September 2014 / Revised: 9 December 2014 / Accepted: 16 December 2014 / Published online: 11 January 2015

Abstract Analyses of four endocrine disrupting chemicals (EDCs) in water and milk samples were undertaken by using magnetic molecularly imprinted polymers (MMIPs). These were prepared via the surface molecular imprinting technique using super paramagnetic core-shell nanoparticle as support. Diethylstilbestrol (DES), which is a typical EDC, was employed as the template molecule. The obtained MMIPs were characterized using transmission electron microscope, Fourier transform infrared, X-ray diffraction, and vibrating sample magnetometer. Accordingly, the adsorption capacity and selectivity of prepared MMIPs were investigated. The binding isotherms were obtained for DES and fitted by the Freundlich isotherm model. A corresponding analytical method to determine four EDCs was developed. The recoveries of the spiked samples in pond water and pure milk range from 67.8 to 93.2 % and from 65.3 to 92.5 %, respectively. Coupled with high-performance liquid chromatography analysis, the prepared MMIPs were successfully applied to the analysis of EDCs in water and milk samples.

Keywords Molecularly imprinted polymers · Super paramagnetic · Endocrine disrupting chemicals · Water and milk

Introduction

Molecularly imprinted polymers (MIPs), featuring high specificity, good stability, ease of preparation, and low cost, are receiving remarkable attention as smart and robust materials for sample preconcentration and separation [1–4]. With tailor-made binding sites, MIPs not only recognize the size and shape of a given template but also respond to the functional groups of the molecule [5, 6]. Successful applications of MIPs have been demonstrated in various fields including chem/biosensors [7, 8], solid phase extraction (SPE) [9–11], environmental analysis [12], pharmaceutical analysis [13], food analysis [14], etc. However, some drawbacks to MIPs have restricted their widespread application, such as incomplete template removal, slow mass transfer, poor site accessibility, irregular shape, or heterogeneous distribution of binding sites [15]. Many efforts have been made to address the above issues. Imparting magnetism to the MIPs and then using magnetic separation is a promising alternative.

Surface imprinted technique, imprinting MIPs on the surface of supporting substrate (e.g., silica particle [16, 17], carbon nanotubes [18, 19], polymer supports [20, 21], and magnetic nanoparticles [22, 23]), is becoming one of the most effective ways to improve the MIPs preparation. Surface imprinted polymers reveal high binding capacities, fast mass transfer, and rapid binding kinetics due to the easy accessibility to recognition sites and the homogeneous distribution of binding sites [24]. Notably, the MIPs with magnetic property are superior for easy handling and fast separation from the matrix using an external magnetic field without additional centrifugation or filtration [25]. The magnetic molecularly imprinted polymers (MMIPs), which have already been prepared in some works [26–29], also display higher adsorption ability and excellent recognition selectivity.

Endocrine disrupting chemicals (EDCs) are exogenous substances with the potential to elicit adverse effects on the normal endocrine function, and consequently have drawn extensive scientific, societal, and political attention [30]. Among the EDCs identified so far, diethylstilbestrol (DES), hexestrol (HES), and dienestrol (DIS) are often studied as a

Electronic supplementary material The online version of this article (doi:10.1007/s00216-014-8425-0) contains supplementary material, which is available to authorized users.

X. Xie · X. Pan · S. Han · S. Wang (✉)
School of Pharmacy, Health Science Center, Xi'an Jiaotong University, 710061 Xi'an, China
e-mail: wangsc@mail.xjtu.edu.cn

group of synthetic estrogens because of their structural and estrogenic similarities [31], which used to prevent spontaneous abortion clinically. However, the long-term intake of synthetic estrogens can cause tumors such as breast cancer and prostate cancer [32, 33]. For the purpose of fattening animals, large amounts of synthetic estrogens are illegally used which can then be excreted to milk or discharged into the aquatic environment [31]. Bisphenol A (BPA) is also a typical EDCs which can potentially interfere with the endocrine system of wildlife and humans and increase cancer incidence. BPA has been widely used for the production of polycarbonates plastics and epoxy resins; it is inevitably released from many plastic packages, such as plastic drinking bottles, leading to food pollution [34]. Thus, development of highly sensitive and selective methodologies for determination of the four EDCs is of great significance for food safety supervision. Several MIPs have been prepared for the enrichment and detection of EDCs [31, 35–37] and endogenous estrogen [38, 39]. The application of the merits of magnetic supporting substrate for the construction of MIPs of DES has not been reported yet.

In this work, the MMIPs were successfully developed for the analysis of four EDCs in water and milk samples. DES was used as the template and super paramagnetic core-shell nanoparticle as supporter. The characterization, adsorption capacity, and selectivity were investigated. The operation conditions affecting the extraction of the four EDCs by MMIPs were optimized, and the analytical performance of the method was evaluated. To demonstrate the applicability, the developed method was applied to the analysis of the four EDCs in real-world samples of pond water and pure milk.

Experimental procedures

Chemicals

DES, HES, DIS, BPA, and paeonol (PN) (Electronic Supplementary Material (ESM) Fig. S1) were obtained from Aladdin Reagent Co., Ltd. (Shanghai, China). Acrylamide (AA), methylacrylic acid (MAA), ethylene glycol dimethacrylamide (EGDMA), 2,2′-azobisissobutyronitrile (AIBN), and 3-(trimethoxysilyl)propyl methacrylate (MPS) were purchased from J&K Scientific Co., Ltd. (Beijing, China). Ferric chloride ($FeCl_3{\cdot}6H_2O$) and ferrous chloride ($FeCl_2{\cdot}4H_2O$) were purchased from Tianjin Tianli Chemicals Co., Ltd. (Tianjin, China). Tetraethoxysilane (TEOS), isopropanol, anhydrous toluene, and ammonium hydroxide (28 %, weight percent) were supplied from Tianjin Chemical Reagent Co., Ltd. (Tianjin, China). HPLC-grade acetonitrile and methanol were from Merck Co. Ltd. (Darmstadt, Germany). Ultra-pure water was prepared with the FLOM purification system (Shandong, China).

Instruments

Transmission electron microscope (TEM) images were obtained with a Hitachi-600 TEM (Tokyo, Japan). The Fourier transform infrared (FT-IR) spectra were recorded on a Nicolet Nexus-670 FT-IR spectrometer (Madison, USA). All the spectra were collected in the range of 4,000–500 cm^{-1}. The crystal structures were characterized by a Bruker D8 Advance X-ray diffraction (XRD) using Cu $K\alpha$ radiation (Bremen, Germany). The magnetic properties were measured using an Mpms Squid vibrating sample magnetometer (VSM) (San Diego, USA). Chromatographic analysis was carried out on Shimadzu LC-20A HPLC system equipped with diode array detection (DAD) system (Kyoto, Japan). A reversed phase C_{18} column (150 mm×4.6 mm i.d., 5 μm) was obtained from Thermo Fisher Scientific Co., Ltd. (Madison, USA). The mobile phase consisted of water and methanol (42:58, *v*/*v*) with the flow rate of 1.0 mL min^{-1}. The injection volume and detection wavelength were 10 μL and 230 nm, respectively [35].

Preparation of the MMIPs

The preparation protocol was shown in ESM Fig. S2. At first, Fe_3O_4 nanoparticles were prepared by coprecipitation. Briefly, 8.1 g of $FeCl_3{\cdot}6H_2O$ and 4.0 g of $FeCl_2{\cdot}4H_2O$ were dissolved in 160 mL of deoxygenated water under stirring at 500 rpm under nitrogen. One hundred milliliter of ammonium hydroxide was dropwise added into the solution, and the reaction was maintained at 80 °C for 30 min [40]. The black precipitates were collected by magnetic separation, washed with ultra-pure water until the pH of the washings became neutral, and finally dried under vacuum at 60 °C for 24 h. Then 600 mg of Fe_3O_4 nanoparticles were dispersed in 50 mL of isopropanol and 10 mL of ultra-pure water by ultra sonication for 30 min, followed by the addition of 20 mL of ammonium hydroxide and 8 mL of TEOS. The mixtures were reacted for 12 h at room temperature with stirring at 500 rpm [41]. The obtained $Fe_3O_4@SiO_2$ nanoparticles were dried under vacuum at 60 °C and then modified with MPS. The detailed procedures were as follows: 1 g of $Fe_3O_4@SiO_2$ nanoparticles were dispersed in 100 mL of anhydrous toluene containing 10 mL of MPS, and the mixture was reacted at 90 °C for 24 h under dry nitrogen. After magnetic separation, washing by anhydrous toluene and methanol and drying under vacuum at 60 °C, the surface-modified magnetic particles ($Fe_3O_4@SiO_2$-MPS) were obtained.

The MMIPs were prepared based on surface-imprinted polymerization method. DES (53.6 mg) as the template and 68 μL of MAA as the functional monomer were dissolved in 32 mL of acetonitrile. The mixture was stored in dark for 12 h at room temperature. Then, 200 mg of $Fe_3O_4@SiO_2$-MPS nanoparticles was added into the mixture and stirred for 2 h. Subsequently, 754 μL of cross-linker EGDMA and 60 mg of

initiator AIBN were added into the system, and the mixture was degassed in an ultrasonic bath for 30 min. After filled with nitrogen for 10 min to remove oxygen, the polymerization was performed at 60 °C with nitrogen protection for 24 h. The polymers were collected magnetically, and the template molecule was removed by washing with methanol/acetic acid (9:1, *v*/*v*) and methanol until no DES absorption was detected by HPLC. Finally, the obtained particles (MMIPs) were dried under vacuum at 60 °C. For comparison, the magnetic non-imprinted polymers (MNIPs) were prepared by the same method without the addition of template DES.

Binding experiment

To measure the adsorption capacity, 20 mg of MMIPs or MNIPs was equilibrated with 1 mL various concentrations of DES standard solution (10–160 μg mL^{-1} in acetonitrile), respectively. The samples were shaken in Zhengji incubator (Jiangsu, China) for 24 h at 25 °C. Then the MMIPs or MNIPs were magnetically separated from the solution, and the remained DES in solution was analyzed by HPLC. The adsorption capacity (Q, μg g^{-1}) was calculated following the equation:

$$Q = (C_i - C_e) \times \frac{V}{m} \quad (1)$$

where C_i and C_e (μg mL^{-1}) are the initial and equilibrium concentrations of the analytes, respectively. V (mL) is the volume of solution, and m (g) is the mass of polymers.

Selectivity evaluation

Twenty milligrams of MMIPs or MNIPs was equilibrated with 1 mL of DES, the structurally similar compounds HES, DIS, and BPA, or the reference compound PN solution (20 μg mL^{-1} in acetonitrile) to evaluate the selectivity. Competitive recognition studies were performed with 1 mL mixed solution of DES and PN (20 μg mL^{-1} for each in acetonitrile). The extraction and analysis procedures were then conducted as described earlier in "Binding experiment".

The interrelated absorbed coefficient was evaluated by the following equations:

$$K_d = \frac{Q}{C_e} \quad (2)$$

where K_d is the distribution coefficient. Q and C_e are as described previously.

$$K = \frac{K_{d1}}{K_{d2}} \quad (3)$$

where K is the selectivity coefficient. K_{d1} and K_{d2} are the distribution coefficient of target and competitive molecules, respectively.

$$K' = \frac{K_{MMIPs}}{K_{MNIPs}} \quad (4)$$

where K' is the relative selectivity coefficient. K_{MMIPs} and K_{MNIPs} represent the selectivity coefficient of MMIPs and MNIPs, respectively.

Application of the MMIPs to real samples

Pond water was from Northwestern Polytechnical University (Xi'an, China), and five batches of pure milk were purchased from a supermarket in Xi'an, China. The samples were packed in plastic bottles and stored in dark at 4 °C.

Without any pretreatment, 20 mg of MMIPs or MNIPs was added to the spiked pond water (1 mL), respectively, and shook at 25 °C for 30 min. The polymers were magnetically separated from the solution (ESM Fig. S3). After the supernatant solution was discarded, the collected polymers were washed with 1 mL acetonitrile. Finally, the polymers were eluted with 1 mL of methanol/acetic acid (9:1, *v*/*v*) by ultra sonication for 20 min. The supernatant (0.5 mL) was completely evaporated and dissolved in 0.1 mL of acetonitrile for further HPLC analysis.

Because milk is complex, it is essential to remove its lipids and proteins before the MMIPs adsorption. In this study, acetonitrile was used for protein precipitation. Five milliliters of spiked pure milk was carried out by adding 5 mL of acetonitrile to precipitate protein. The mixture was oscillated and centrifuged at 10,000 rpm for 10 min. The supernatant was centrifuged twice and pooled together. Then 20 mg of MMIPs or MNIPs was added to the supernatant (1 mL), respectively. The other operational processes were the same as the procedure of water samples.

Results and discussion

Preparation of MMIPs

The obtained MMIPs were prepared by surface molecules polymerization technology. Fe_3O_4 nanoparticles were firstly synthesized by coprecipitation reaction. Secondly, the surface of Fe_3O_4 nanoparticles was coated with silica to provide a biocompatible and hydrophilic surface, and prevent oxidation. Furthermore, silanol groups were beneficial to chemical modification on the surface of Fe_3O_4@SiO_2 nanoparticles. After that, double bonds were introduced onto the surface of Fe_3O_4@SiO_2 nanoparticles with MPS for reaction with EGDMA to initiate the copolymerization of DES and MAA on the Fe_3O_4@SiO_2 surface in the presence of AIBN.

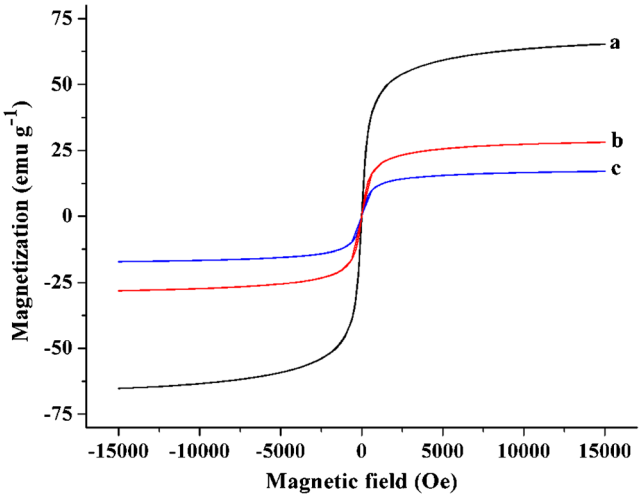

Fig. 1 VSM curves of Fe_3O_4 (**a**), Fe_3O_4@SiO_2 (**b**), and MMIPs (**c**)

In order to obtain MMIPs with the highest recognition capability, some essential factors were investigated during the preparation procedure. As known, solvent plays an important role as a porogen and dissolvent in the preparation of the non-covalent type molecularly imprinted polymer. Weak polarity solvent is usually selected as the optimal condition because of non-covalent molecular recognition. In consideration of the weak polarity and excellent dissolving capacity, acetonitrile was selected as the porogen. The generation of recognition sites was dependent on the functional monomer through organized self-assembly with the template. In this study, AA and MAA were selected to evaluate the specific recognition ability of MMIPs for DES. The results indicated that using MAA had better molecular recognition. The optimization of mole ratio of template to functional monomer was a critical factor that eventually led to a maximum high-affinity binding sites in the synthesized MMIPs. Three molar ratios of the template DES to the functional monomer MAA of 1:3, 1:4, and 1:5 were investigated. The optimum ratio of functional monomer to cross-linker was 1:5 according to previous reports [3]. The results indicated that the optimum molar ratio of template/MAA/EGDMA was 1:4:20 to prepare MMIPs for DES.

Table 1 Freundlich fitting parameters, number of binding sites ($N_{kmin-kmax}$), and weighted average affinity ($K_{kmin-kmax}$) for DES on the MMIPs and MNIPs

	MMIPs	MNIPs
$N_{kmin-kmax}$ (mg g^{-1})	3.086±0.009	0.933±0.006
K_f [(mg g^{-1})(mL μg^{-1})^n]	0.779	0.102
$K_{kmin-kmax}$ (mL μg^{-1})	0.102±0.004	0.011±0.001
K_{range} (mL μg^{-1})	0.014–0.625	0.008–0.083
n	0.4196	0.6094
r	0.9961	0.9705

[a] Data are shown as means±S.D.

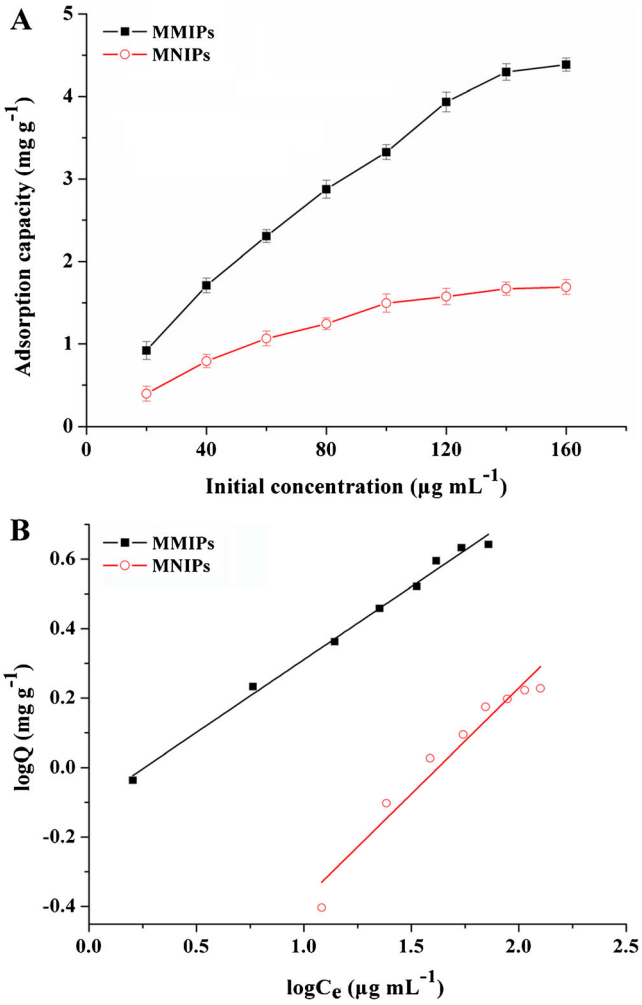

Fig. 2 **A** Adsorption isotherm curve of MMIPs and MNIPs; **B** Freundlich analysis curves of MMIPs and MNIPs

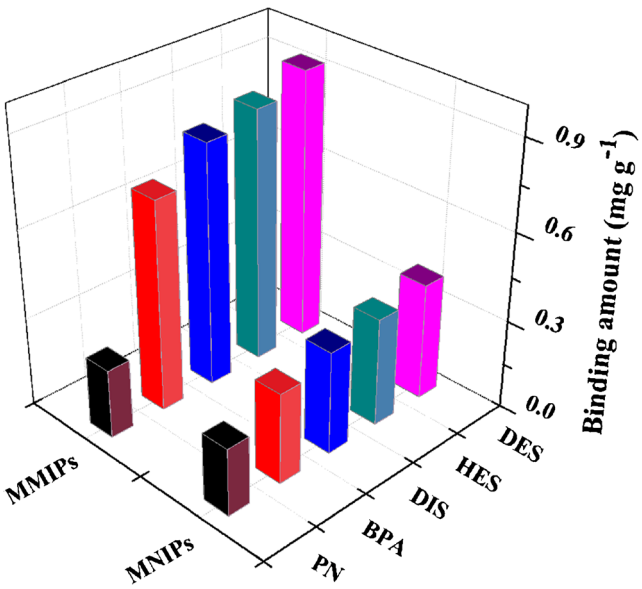

Fig. 3 The specific binding behaviors of MMIPs and MNIPs for four EDCs and PN

Characterization of MMIPs

The particle morphology of Fe_3O_4@SiO_2 and MMIPs can be obviously observed by TEM (ESM Fig. S3). It can be seen that the core-shell structure of Fe_3O_4@SiO_2 is about 230 nm in size. After imprinting process, the MMIPs still revealed the fine core-shell structure with the diameter of 250 nm, which suggested that imprinted layer was well distributed on the surface of Fe_3O_4@SiO_2.

FT-IR spectra of Fe_3O_4, Fe_3O_4@SiO_2, Fe_3O_4@SiO_2-MPS, MMIPs, and MNIPs are shown in ESM Fig. S4. The strong absorption peak at about 579 cm^{-1} was characteristic of Fe-O vibration, and the strong peak around 1,099 cm^{-1} (Si–O asymmetric stretching vibration), and 799 cm^{-1} (Si–O symmetric stretching vibration) displayed that SiO_2 was successfully encapsulated onto the surface of Fe_3O_4 nanoparticles. The C–H stretching vibration peak at 2,930 cm^{-1} indicated that MPS groups were indeed coated onto the surfaces of the Fe_3O_4@SiO_2 nanoparticles. No obvious differences were found between the spectra of MMIPs and MNIPs. The new absorbance peak of C=O at 1,733 cm^{-1} for EDGMA showed that the polymerization was successful. Moreover, the peak intensity in the MNIPs was lower than that in MMIPs because of the effect of hydrogen between DES and MAA.

The structural properties of Fe_3O_4, Fe_3O_4@SiO_2, and MMIPs were analyzed by XRD. As shown in ESM Fig. S5, six characteristic peaks marked by their indices (220, 311, 400, 422, 511, and 440) were obtained in the 2θ region of 20–80°. The discernible peaks matches well with the database of magnetite in JCPDS (JCPDS card: 19–629) file. This finding proved that the synthesis process did not change the XRD phase of Fe_3O_4.

VSM was employed to characterize the magnetic properties of the obtained magnetic materials, and their VSM magnetization curves are shown in Fig. 1. Based on the VSM data, the supporting core (Fe_3O_4) exhibits a saturation magnetization value of 65.30 emu g^{-1}. The saturation magnetizations of Fe_3O_4@SiO_2 and MMIPs decreased after the formation of the polymeric coating (28.09 emu g^{-1} for Fe_3O_4@SiO_2 and 17.11 emu g^{-1} for MMIPs). These magnetic properties enabled magnetic separation with a common magnet.

Table 2 The selectivity parameters of MMIPs and MNIPs (n=3)

	C_e (μg mL^{-1})		Q (mg g^{-1})		K_d (mL g^{-1})		K	K'
	DES	PN	DES	PN	K_{d1} (DES)	K_{d2} (PN)		
MMIPs	1.66	15.43	0.92	0.23	552.41	14.81	37.30	15.15
MNIPs	12.19	15.87	0.39	0.21	32.03	13.01	2.46	

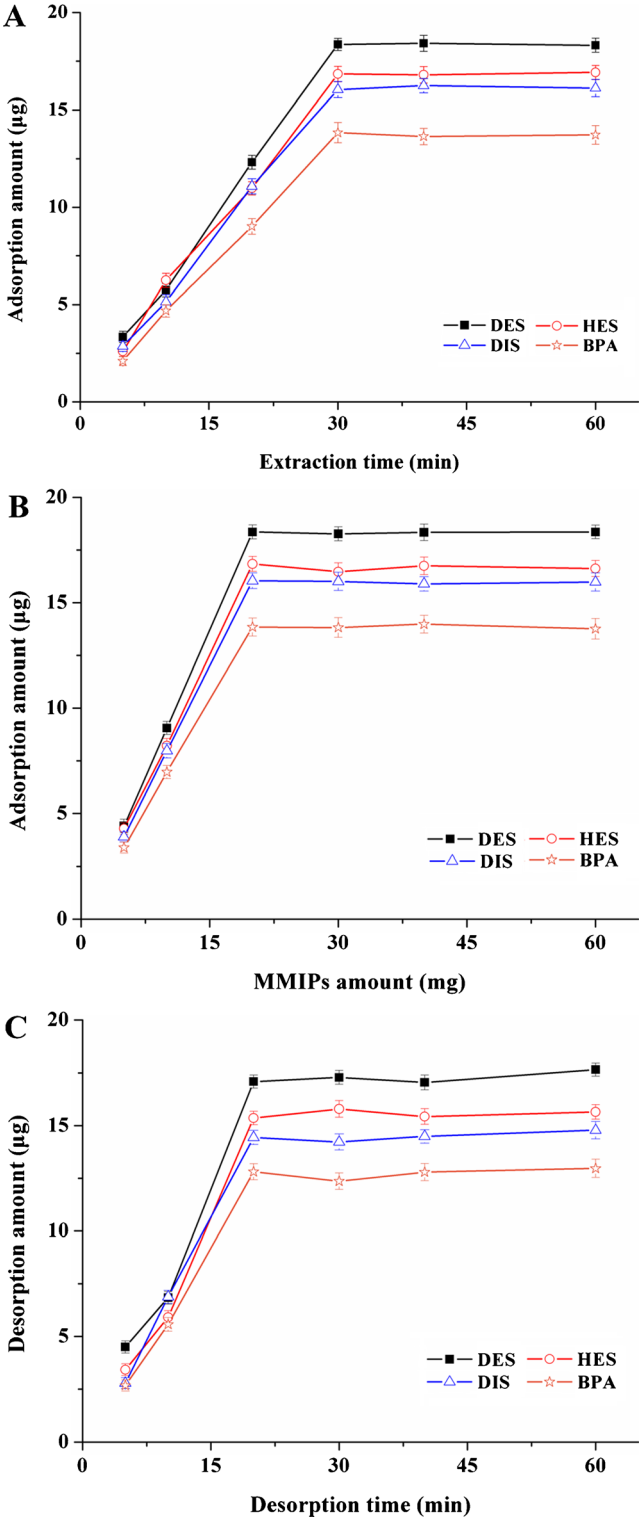

Fig. 4 **A** Extraction time curves; **B** MMIPs amount curves; and **C** desorption time curves of MMIPs coating to the four EDCs mixed standard solution

Binding isotherms and Freundlich analysis

The adsorption capacity was performed by subjecting the MMIPs or MNIPs to various initial concentrations of DES.

As shown in Fig. 2A, the amount of DES adsorbed increases along with the initial concentration; when the initial concentration of DES was 140 μg mL^{-1}, the binding amount achieved a nearly saturated plateau. The MMIPs revealed highly specific binding ability to the template DES than MNIPs.

In order to further study the binding properties of MMIPs and MNIPs, the obtained data were analyzed using the Freundlich isotherm model equation [3]:

$$\log Q = n\log C_e + \log K_f \quad (5)$$

where Q and C_e are as described in Eq. (1), and n and K_f are the Freundlich constants related to the binding intensity and binding capacity, respectively. The values of n and K_f could be calculated from plotting $\log Q$ versus $\log C_e$ by a linear regression (Fig. 2B). The parameter n varies from 0 to 1, with 1 being homogeneous and values approaching 0 being increasingly heterogeneous. In addition, the number of binding sites per gram of polymer ($N_{k\min-k\max}$) and the weighted average affinity constant ($K_{k\min-k\max}$) were calculated using the following Eqs. (6) and (7), respectively.

$$N_{k\min-k\max} = K_f\left(1-n^2\right)\left(K_{\min}^{-n}-K_{\max}^{-n}\right) \quad (6)$$

$$K_{k\min-k\max} = \left(\frac{n}{n-1}\right)\left(\frac{K_{\min}^{1-n}-K_{\max}^{1-n}}{K_{\min}^{-n}-K_{\max}^{-n}}\right) \quad (7)$$

where $K_{\min}=1/C_{e\max}$ and $K_{\max}=1/C_{e\min}$. $C_{e\max}$ and $C_{e\min}$ are the experimental maximum and minimum free analyte concentrations, respectively.

These calculated fitting parameters are summarized in Table 1. According to the n value, the MMIPs had a lower value than the MNIPs, which indicated a more heterogeneous group of binding sites. The binding sites of MMIPs for DES measured were 3.086 mg g^{-1} with an affinity constant of 0.102 mL μg^{-1}, while the binding sites 0.933 mg g^{-1} of MNIPs were with an affinity constant of 0.011 mL μg^{-1}. The results indicated that the template molecule displayed an important role in the heterogeneity of the MIPs.

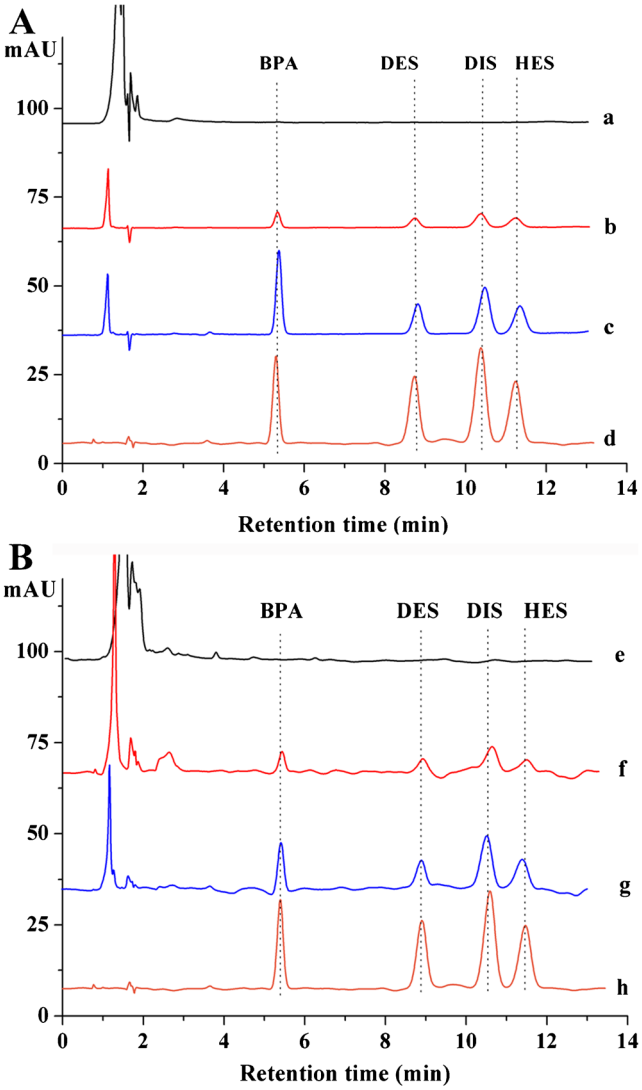

Fig. 5 Chromatograms of (**A**) pond water and (**B**) pure milk: four EDCs spiked extraction solution of sample (*a*, *e*); spiked solution extracted with MNIPs (*b*, *f*); spiked solution extracted with MMIPs (*c*, *g*); four EDCs mixed standard solution (*d*, *h*)

Table 3 Recoveries of the four EDCs after MMIPs extracted of spiked pond water and pure milk (n=3)

	Pond water						Pure milk					
	1 μg mL^{-1}		3 μg mL^{-1}		5 μg mL^{-1}		1 μg mL^{-1}		3 μg mL^{-1}		5 μg mL^{-1}	
	Recovery (%)	RSD (%)	Recovery (%)	RSD (%)	Recovery (%)	RSD (%)	Recovery (%)	RSD (%)	Recovery (%)	RSD (%)	Recovery (%)	RSD (%)
DES	92.3	4.7	92.7	3.2	93.2	5.6	90.4	2.3	92.1	1.6	92.5	2.4
HES	82.6	5.8	83.7	2.4	85.1	3.5	81.2	4.2	82.3	2.3	83.4	2.6
DIS	78.9	3.3	80.2	6.2	82.1	6.4	77.8	3.6	79.2	3.4	79.7	4.8
BPA	67.8	5.6	68.6	4.7	68.9	2.6	65.3	4.8	67.4	4.8	68.2	3.4

Table 4 Analytical results from five batches of pure milk (n=3)

Sample	Batch no.	Protein content (mg mL$^{-)1}$	Fat content (mg mL^{-1})	Carbohydrate content (mg mL^{-1})	DES content (ng mL^{-1})	HES content (ng mL^{-1})	DIS content (ng mL^{-1})	BPA content (ng mL^{-1})
A	6904007601014	30	35	48	Found[a]	Unfound	Unfound	Unfound
B	6910442945187	24	29	60	Unfound	Unfound	Unfound	Unfound
C	6907992501468	30	35	50	Unfound	Unfound	Unfound	Unfound
D	6925572320094	23	25	48	Unfound	Unfound	Unfound	Unfound
E	6923644261405	24	30	68	Unfound	Unfound	Unfound	Unfound

[a] DES could be found, but could not be quantified

Adsorption specificity

To evaluate the specificity of the MMIPs, DES, some analogues (HES, DIS, and BPA), and a reference compound (PN) were selected, and the results were shown in Fig. 3. The adsorption capacities of the MMIPs for the four EDCs are obtained at the range of 0.71–0.92 mg g^{-1}, which is significantly higher than the MNIPs (0.31–0.40 mg g^{-1}). It illustrated that the MMIPs had high specificity for DES and its analogues. Meanwhile, the adsorption capacity of the MMIPs for the four EDCs is significantly higher than PN (0.23 mg g^{-1}), and there was no obvious difference between the MMIPs and MNIPs to adsorb PN (0.22 mg g^{-1} for MNIPs). This indicated that the MMIPs had no specific site to the reference compound with significantly different structures.

The DES and the reference compound PN were selected to act the competitors in competitive assays. The distribution coefficient (K_d), the selectivity coefficient (K), and the relative selectivity coefficient (K') were obtained from these competitive assays. K_d indicates the adsorption ability of a substance, K suggests how selective the sorbent is when it is exposed to two substances, and K' reveals the selective difference between MMIPs and MNIPs [27]. As seen in Table 2, The K value of the MMIPs (37.30) is larger than that of the MNIPs (2.46), indicating that the MMIPs have a higher selectivity for DES over PN. The value of K' is 15.15, confirming that the imprinted polymer has a higher selectivity than the non-imprinted polymer. The MMIPs exhibit a higher affinity for DES due to its template-specific sites, which indicated that the imprinting process significantly improved adsorption selectivity to the imprinted template and no specific site was suited for the reference compound with significantly different structures.

Optimization of extraction procedure

The extraction procedure includes three steps: adsorption, isolation, and desorption. The adsorption time is a key factor in the efficiency of the assay. The effect of the absorption time was conducted in 1 mL mixed solution of four EDCs (20 μg mL^{-1} for each) by varying the shaking time (5–60 min). Figure 4A indicates that the MMIPs (20 mg) reach adsorption equilibrium at approximately 30 min for the four EDCs. Therefore, 30 min extraction time was selected in the following experiments.

Different amounts of MMIPs ranging from 5 to 60 mg in 1 mL mixed solution of four EDCs (20 μg mL^{-1} for each)

Table 5 Comparison of the limits of detection (LOD) with other methods

Extraction method	Detection	Matrix	Compounds	LOD (ng mL^{-1})	Reference
Dual cloud point	MEKC-UV	Water	DES	8.9	[31]
			HES	7.9	
			DIS	8.2	
Stir bar sorptive	HPLC-UV	Pork	DES	0.57	[35]
			HES	0.27	
			DIS	0.21	
MIPs	HPLC-UV	Fish	DES	60	[42]
Hollow fiber tube MIPs	HPLC-UV	Milk	DES	2.5	[43]
			HES	3.3	
			DIS	3.3	
Nanoattapulgite MIPs	HPLC-UV	Water	DES	3.0	[44]
MMIPs	HPLC-UV	Water/milk	DES	3.6/6.3	This work
			HES	6.7/14.6	
			DIS	5.4/12.2	
			BPA	9.5/19.7	

were applied. The extraction time was 30 min. Figure 4B shows that 20 mg was enough for the extraction. Therefore, the amounts of adsorbent were set at 20 mg.

To obtain desorption time of the four EDCs, different time intervals (5–60 min) were evaluated. As shown in Fig. 4C, 20 min is sufficient to accomplish desorption period. Therefore, 20 min was selected in the desorption experiments.

Real sample analysis

A method based on MMIPs coupled to HPLC was established. Analytical performance characteristics such as linearity, limit of detection (LOD), limit of quantification (LOQ), and the recovery were studied. The LOD and LOQ were defined as 3 and 10 times of the signal to noise ratio, respectively. The recovery was estimated by adding known amount of the four EDCs standards into accurately measured pond water or pure milk and then extracted and analyzed.

The developed method was applied to determine the four EDCs in pond water. Good linearity was achieved in the range of 0.02–8.0 μg mL^{-1} for DES and HES, and 0.01–6.0 μg mL^{-1} for DIS and BPA. The correlation coefficient (r) was in the range of 0.9994–0.9996. The LOD were in the range of 3.6–9.5 ng mL^{-1}, and the LOQ were in the range of 10.4–29.8 ng mL^{-1}. The pond water was spiked at three concentration levels. The results are summarized in Table 3. The recoveries of the spiked samples for the four EDCs range from 67.8 to 93.2 % with the RSD values ranging from 2.4 to 6.4 %. The blank pond water was extracted with MMIPs, but the four EDCs were not found. As shown in Fig. 5A, it can be seen that no peaks of EDCs occurred when the spiked pond water (0.5 μg mL^{-1}) was directly detected without MMIPs pre-enrichment, owing to the low spiked concentration of EDCs. No selective peak was observed in the analysis of the spiked sample extracted by MNIPs. After the spiked sample was extracted with MMIPs, the EDCs were concentrated, resulting in the obvious peaks of EDCs exhibited in Fig. 5c. The baseline obtained for the analysis of extracts by MMIPs was as clean as that shown in Fig. 5d for the standard solution. These results indicated that the prepared MMIPs can be utilized to directly and effectively separate and enrich EDCs in water sample.

It was further applied to analyze EDCs in pure milk. Good linearity was achieved in the range of 0.04–8.0 μg mL^{-1} for DES and HES, and 0.02–6.0 μg mL^{-1} for DIS and BPA. The correlation coefficient (r) was in the range of 0.9992–0.9996. The LOD were in the range of 6.3–19.7 ng mL^{-1}, and the LOQ were in the range of 19.2–67.9 ng mL^{-1}. The standard addition method was used to evaluate the repeatability, accuracy, and recovery of the MMIP-HPLC extraction process. The pure milk was spiked with the four EDCs at three concentration levels. The results are summarized in Table 3. The recoveries of the spiked samples for the four EDCs range from 65.3 to 92.5 % with the RSD values ranging from 2.3 to 4.8 %. The four EDCs were not found in blank pure milk. As shown in Fig. 5B, it can be seen that no peaks of EDCs occurred when the four EDCs spiked pure milk (1 μg mL^{-1}) was directly detected without MMIPs pre-enrichment. No selective peak was observed in the analysis of the spiked sample extracted by MNIPs. After the spiked sample was extracted with MMIPs, the EDCs were concentrated, resulting in the obvious peaks of EDCs exhibited in Fig. 5g. The baseline obtained for the analysis of extracts by MMIPs was as clean as that shown in Fig. 5h for the standard solution. In addition, the proposed procedure was applied to analyze five batches of pure milk produced by different manufactures. Results in Table 4 indicated that DES was only found in sample A, but could not be quantified. These results also demonstrated that the prepared MMIPs can be utilized to effectively separate and enrich EDCs in milk samples.

A comparison of LOD obtained by the developed method with those obtained by other methods is summarized in Table 5. As can be seen, the LOD of the developed method was lower than those of Dual cloud point [31] and MIPs [42], similar to those of Hollow fiber tube MIPs [43] and Nanoattapulgite MIPs [44], and high than that of Stir bar sorptive [35]. These results demonstrated that the MMIPs had high selectivity and enrichment ability for the analysis of four EDCs in complex matrix.

In conclusion, on the basis of the surface imprinting strategy, the novel MMIPs nanoparticles were prepared for the analysis of EDCs. The obtained MMIPs were characterized via TEM, FT-IR, XRD, and VSM. The surface imprinted MMIPs showed high binding capacity, short absorption equilibrium time, and specific recognition toward EDCs. The MMIPs nanoparticles also exhibited a desired level of magnetic susceptibility, resulting in the convenient and highly efficient extraction. The MMIPs nanoparticles were directly and successfully utilized to extract four EDCs from pond water and pure milk with satisfactory recoveries and reproducibility. The well-constructed core-shell MMIPs nanoparticles reveal the great prospect for enrichment and separation of such EDCs in complicated matrixes.

Acknowledgments This work was financially supported by National Natural Science Foundation of China (81227802), the China Postdoctoral Science Foundation (2014 M550501), and the Fundamental Research Funds for the Central Universities (xjj2014066).

References

1. Ahmadi F, Yawari E, Nikbakht M (2014) Computational design of an enantioselective molecular imprinted polymer for the solid phase extraction of S-warfarin from plasma. J Chromatogr A 1338:9–16

2. Blasco B, Pico Y (2012) Development of an improved method for trace analysis of quinolones in eggs of laying hens and wildlife species using molecularly imprinted polymers. J Agric Food Chem 60:11005–11014
3. Chen FF, Wang R, Shi YP (2012) Molecularly imprinted polymer for the specific solid-phase extraction of kirenol from *Siegesbeckia pubescens* herbal extract. Talanta 89:505–512
4. Sadeghi S, Jahani M (2013) Selective solid-phase extraction using molecular imprinted polymer sorbent for the analysis of Florfenicol in food samples. Food Chem 141:1242–1251
5. Vlatakis G, Andersson LI, Muller R, Mosbach K (1993) Drug assay using antibody mimics made by molecular imprinting. Nature 361: 645–647
6. Wulff G (2002) Enzyme-like catalysis by molecularly imprinted polymers. Chem Rev 102:1–27
7. Tiwari MP, Prasad BB (2014) An insulin monitoring device based on hyphenation between molecularly imprinted micro-solid phase extraction and complementary molecularly imprinted polymer-sensor. J Chromatogr A 1337:22–31
8. Barrios CA, Zhenhe C, Navarro-Villoslada F, Lopez-Romero D, Moreno-Bondi MC (2011) Molecularly imprinted polymer diffraction grating as label-free optical bio(mimetic)sensor. Biosens Bioelectron 26:2801–2804
9. Rodriguez E, Navarro-Villoslada F, Benito-Pena E, Marazuela MD, Moreno-Bondi MC (2011) Multiresidue determination of ultratrace levels of fluoroquinolone antimicrobials in drinking and aquaculture water samples by automated online molecularly imprinted solid phase extraction and liquid chromatography. Anal Chem 83:2046–2055
10. Pakade V, Lindahl S, Chimuka L, Turner C (2012) Molecularly imprinted polymers targeting quercetin in high-temperature aqueous solutions. J Chromatogr A 1230:15–23
11. Xu SX, Zhang XF, Sun YH, Yu D (2013) Microwave-assisted preparation of monolithic molecularly imprinted polymeric fibers for solid phase microextraction. Analyst 138:2982–2987
12. Li Y, Li X, Chu J, Dong CK, Qi JY, Yuan YX (2010) Synthesis of core-shell magnetic molecular imprinted polymer by the surface RAFT polymerization for the fast and selective removal of endocrine disrupting chemicals from aqueous solutions. Environ Pollut 158: 2317–2323
13. Chen FF, Wang GY, Shi YP (2011) Molecularly imprinted polymer microspheres for solid-phase extraction of protocatechuic acid in Rhizoma homalomenae. J Sep Sci 34:2602–2610
14. Ramstrom O, Skudar K, Haines J, Patel P, Bruggemann O (2001) Food analyses using molecularly imprinted polymers. J Agric Food Chem 49:2105–2114
15. Chen LX, Xu SF, Li JH (2011) Recent advances in molecular imprinting technology: current status, challenges and highlighted applications. Chem Soc Rev 40:2922–2942
16. Wang XY, Kang Q, Shen DZ, Zhang Z, Li JH, Chen LX (2014) Novel monodisperse molecularly imprinted shell for estradiol based on surface imprinted hollow vinyl-SiO_2 particles. Talanta 124:7–13
17. Chen HC, Yuan DY, Li YY, Dong MJ, Chai ZH, Kong J, Fu GQ (2013) Silica nanoparticle supported molecularly imprinted polymer layers with varied degrees of crosslinking for lysozyme recognition. Anal Chim Acta 779:82–89
18. Yang WJ, Jiao FP, Zhou L, Chen XQ, Jiang XY (2013) Molecularly imprinted polymers coated on multi-walled carbon nanotubes through a simple indirect method for the determination of 2,4-dichlorophenoxyacetic acid in environmental water. Appl Surf Sci 284:692–699
19. Puoci F, Hampel S, Parisi OI, Hassan A, Cirillo G, Picci N (2013) Imprinted microspheres doped with carbon nanotubes as novel electroresponsive drug-delivery systems. J Appl Polym Sci 130: 829–834
20. Xu WZ, Zhou W, Xu PP, Pan JM, Wu XY, Yan YS (2011) A molecularly imprinted polymer based on TiO_2 as a sacrificial support for selective recognition of dibenzothiophene. Chem Eng J 172:191–198
21. Wang XH, Chen LR, Xu XJ, Li YZ (2011) Synthesis of molecularly imprinted polymers via ring-opening metathesis polymerization for solid-phase extraction of bisphenol A. Anal Bioanal Chem 401: 1423–1432
22. Xie LJ, Jiang RF, Zhu F, Liu H, Ouyang GF (2014) Application of functionalized magnetic nanoparticles in sample preparation. Anal Bioanal Chem 406:377–399
23. Zhao M, Zhang C, Zhang Y, Guo XZ, Yan HS, Zhang HQ (2014) Efficient synthesis of narrowly dispersed hydrophilic and magnetic molecularly imprinted polymer microspheres with excellent molecular recognition ability in a real biological sample. Chem Commun 50: 2208–2210
24. Li DY, He XW, Chen Y, Li WY, Zhang YK (2013) Novel hybrid structure silica/CdTe/molecularly imprinted polymer: synthesis, specific recognition, and quantitative fluorescence detection of bovine hemoglobin. Acs Appl Mater Inter 5:12609–12616
25. Li Y, Ding MJ, Wang S, Wang RY, Wu XL, Wen TT, Yuan LH, Dai P, Lin YH, Zhou XM (2011) Preparation of imprinted polymers at surface of magnetic nanoparticles for the selective extraction of tadalafil from medicines. Acs Appl Mater Inter 3:3308–3315
26. Yao GH, Liang RP, Huang CF, Wang Y, Qiu JD (2013) Surface plasmon resonance sensor based on magnetic molecularly imprinted polymers amplification for pesticide recognition. Anal Chem 85: 11944–11951
27. Kong X, Gao RX, He XW, Chen LX, Zhang YK (2012) Synthesis and characterization of the core-shell magnetic molecularly imprinted polymers (Fe_3O_4@MIPs) adsorbents for effective extraction and determination of sulfonamides in the poultry feed. J Chromatogr A 1245:8–16
28. Wang XH, Fang QX, Liu SP, Chen L (2012) Preparation of a magnetic molecularly imprinted polymer with pseudo template for rapid simultaneous determination of cyromazine and melamine in bio-matrix samples. Anal Bioanal Chem 405:5843–5852
29. Madrakian T, Afkhami A, Mahmood-Kashani H, Ahmadi M (2013) Superparamagnetic surface molecularly imprinted nanoparticles for sensitive solid-phase extraction of tramadol from urine samples. Talanta 105:255–261
30. Vandenberg LN, Colborn T, Hayes TB, Heindel JJ, Jacobs DR, Lee DH, Shioda T, Soto AM, Vom Saal FS, Welshons WV, Zoeller RT, Myers JP (2012) Hormones and endocrine-disrupting chemicals: low-dose effects and nonmonotonic dose responses. Endocr Rev 33:378–455
31. Wen YY, Li JH, Liu JS, Lu WH, Ma JP, Chen LX (2013) Dual cloud point extraction coupled with hydrodynamic-electrokinetic two-step injection followed by micellar electrokinetic chromatography for simultaneous determination of trace phenolic estrogens in water samples. Anal Bioanal Chem 405:5843–5852
32. Giusti RM, Iwamoto K, Hatch EE (1995) Diethylstilbestrol revisited-a review of the long-term health-effects. Ann Intern Med 122:778–788
33. Giese RW (2003) Measurement of endogenous estrogens: analytical challenges and recent advances. J Chromatogra A 1000:401–412
34. Xue JQ, Li DW, Qu LL, Long YT (2013) Surface-imprinted core-shell Au nanoparticles for selective detection of bisphenol A based on surface-enhanced Raman scattering. Anal Chim Acta 777:57–62
35. Hu C, He M, Chen BB, Hu B (2012) Determination of estrogens in pork and chicken samples by stir bar sorptive extraction combined with high-performance liquid chromatography-ultraviolet detection. J Agric Food Chem 60:10494–10500
36. Xia XL, Lai EPC, Ormeci B (2013) Duo-molecularly imprinted polymer-coated magnetic particles for class-selective removal of endocrine-disrupting compounds from aqueous environment. Environ Sci Pollut Res 20:3331–3339

37. Murray A, Ormeci B (2012) Application of molecularly imprinted and non-imprinted polymers for removal of emerging contaminants in water and wastewater treatment: a review. Environ Sci Pollut Res 19:3820–3830
38. Ning FJ, Peng HL, Li JH, Chen LX, Xiong H (2014) Molecularly imprinted polymer on magnetic graphene oxide for fast and selective extraction of 17β-estradiol. J Agric Food Chem 62:7436–7443
39. Lan HZ, Gan N, Pan DD, Hu FT, Li TH, Long NB, Qiao L (2014) An automated solid-phase microextraction method based on magnetic molecularly imprinted polymer as fiber coating for detection of trace estrogens in milk powder. J Chromatogr A 1331:10–18
40. Zhang HF, Shi YP (2012) Magnetic retrieval of chitosan: extraction of bioactive constituents from green tea beverage samples. Analyst 137:910–916
41. Lu FG, Li HJ, Sun M, Fan LL, Qiu HM, Li XJ, Luo CN (2012) Flow injection chemiluminescence sensor based on core-shell magnetic molecularly imprinted nanoparticles for determination of sulfadiazine. Anal Chim Acta 718:84–91
42. Jiang XM, Zhao CD, Jiang N, Zhang HX, Liu MC (2008) Selective solid-phase extraction using molecular imprinted polymer for the analysis of diethylstilbestrol. Food Chem 108:1061–1067
43. Liu MH, Li MJ, Qiu B, Chen X, Chen GN (2010) Synthesis and applications of diethylstilbestrol-based molecularly imprinted polymer-coated hollow fiber tube. Anal Chim Acta 663:33–38
44. Zhao CD, Ji YS, ShaoYL JXM, Zhang HX (2009) Novel molecularly imprinted polymer prepared by nanoattapulgite as matrix for selective solid-phase extraction of diethylstilbestrol. J Chromatogr A 1216: 7546–7552